

Porcelain tile microstructure: Implications for polished tile properties

E. Sánchez^{a,*}, M.J. Ibáñez^a, J. García-Ten^a, M.F. Quereda^a, I.M. Hutchings^b, Y.M. Xu^b

^a Instituto de Tecnología Cerámica, Asociación de Investigación de las Industrias Cerámicas, Universitat Jaume I, Castellón, Spain

^b Institute for Manufacturing, University of Cambridge, Mill Lane, Cambridge CB2 1RX, UK

Received 21 January 2005; received in revised form 19 April 2005; accepted 5 June 2005

Available online 27 July 2005

Abstract

The present study was undertaken to determine the influence of sintered porcelain tile microstructure on mechanical properties (fracture strength, modulus of elasticity and fracture toughness) and surface properties (gloss and stain resistance). To obtain sintered specimens with different microstructures the peak firing temperature was varied for bodies made with industrial spray-dried powder, and sets of test compositions were also made in which quartz content and quartz particle size were varied.

Liquid-phase sintering is the typical densification mechanism involved in the achievement of minimum porosity, which is characterised by isolated round pores. Bloating occurred above the firing temperature for minimum porosity. Increases in quartz content and quartz particle size in the starting composition led to reduced body sinterability, and thus gave rise to higher porosity in the fired tile.

Mechanical properties were adversely affected by an increase in fired tile porosity. For the same variation in porosity, mechanical properties were more sensitive to the change in quartz content than to changes in particle size. No toughening effect was observed with a rise in quartz content or a decrease in particle size: mechanical properties depended primarily on sintered specimen porosity.

Gloss and stain resistance (which characterise polished surface quality) varied with surface porosity, both showing the highest values for lowest porosity. The relationship between porosity and gloss was close to linear.

© 2005 Elsevier Ltd. All rights reserved.

Keywords: Microstructure final; Surfaces; Mechanical properties; Traditional ceramics; Tiles; Porosity

1. Introduction

Recently there has been a strong increase in polished porcelain tile manufacture. The manufacturing process yields ceramic tiles with good mechanical and chemical properties. The last process phase, the polishing step, serves to produce a very smooth, glossy surface finish that could not be achieved without the polishing treatment. A key product characteristic is the near-zero water absorption (typically less than 0.5%), which helps make the porcelain tile a high-performance material. The tiles thus have high fracture strength as well as good chemical, stain and frost resistance, enabling them to be used in any environment.

The product consists of a glassy matrix of a feldspathic nature, containing disperse crystalline phases such as quartz and mullite. Mullite is typically found in low quantities (up to ~8%) because of the starting composition characteristics and the fast firing cycle and low firing temperature used in porcelain tile manufacture.¹ The major crystalline phase is quartz, which can amount to 30 wt% or more in the fired body, with a maximum particle size generally <45 μm as a result of industrial milling. It is therefore not surprising that porcelain tile microstructure is largely defined by quartz content and characteristics.²

The technical characteristics of porcelain tiles are intimately related to the porosity of the fired product. While the high fracture strength is a result of low total porosity, the frost resistance depends on the near-zero apparent surface porosity, which makes the tile impervious to frost-thaw cycles. The surface properties of the polished product, such as gloss or

* Corresponding author.

E-mail address: esanchez@itc.uji.es (E. Sánchez).

stain resistance, also depend on the level of surface porosity resulting from the polishing process.³ In the case of stain resistance, pore size and geometry influence surface soilability and cleanability.^{4,5}

Porcelain tile properties have to date received little scientific attention, despite the commercial significance of this product and its high potential performance. Greater knowledge of porcelain tile properties and of the relation between these properties and the microstructure is needed to design improved compositions and manufacturing processes. In the present work, porcelain tile microstructure has been modified in a systematic manner to study its influence on the key properties of surface quality (gloss and stain resistance) and mechanical properties (fracture strength, Young's modulus and toughness). The variation in microstructure was obtained by varying the peak firing temperature, and by the use of compositions with different quartz contents and quartz particle size.

2. Materials and experimental methods

2.1. Materials

Two types of compositions were used. The first type consisted of typical industrial spray-dried powder used in porcelain tile manufacture, formulated from a mixture of ball clays, quartz and sodium feldspar. The second type was a laboratory composition which comprised similar raw materials as the industrial type in which quartz content and particle size were varied. This second type of composition was prepared in the laboratory because the desired compositional range was not available in an industrial powder.

Table 1 lists the laboratory compositions whose quartz content was modified (designated with the codes A–E). The mean quartz particle size in this series was 20.4 μm . A further series of laboratory compositions was prepared, based on composition C, in which quartz particle size was modified (Table 2, codes F–I). Further data for these compositions have been reported elsewhere.⁶

Table 1

Laboratory compositions in which quartz content was varied (raw material contents in wt%)

Composition	A	B	C	D	E
Clay	35	32.8	30.6	26.2	17.5
Feldspar	55	51.6	48.1	41.2	27.5
Talc	10	9.4	8.8	7.5	5
Quartz	0	6.25	12.5	25	50

Table 2

Laboratory compositions in which quartz particle size was varied (all containing 12.5 wt% added quartz)

Composition	F	G	H	I
Mean particle size, d_{50} (μm)	42.5	23.5	13.4	3.4

The quartz content of typical standard industrial compositions ranges from 20 to 30 wt%, and the mean quartz particle size in these compositions usually lies between 10 and 15 μm . The quartz content and particle size ranges analysed in the test compositions therefore fully cover the range encountered in industrial practice.

2.2. Experimental methods

Each composition was used to form cylindrical test specimens (about 7 mm thick and 50 mm in diameter) and prism-shaped test specimens (80 mm long, 20 mm wide and about 7 mm thick) by uniaxial pressing, at a moisture content of 5.5 wt% (dry weight basis) and pressure of 350 kg/cm^2 . After drying, the specimens were fired in an electric laboratory kiln at the maximum densification temperature which had been established previously from the vitrification diagram, determined from the bulk density of fired specimens.⁷ Some characteristics of the firing cycle were: heating rate 25 $^{\circ}\text{C}/\text{min}$, 6-min hold at maximum temperature and a total cool-to-cool cycle of 60 min. The procedure basically consists of determining the vitrification diagram (variation of bulk density as a function of firing temperature) for each composition. The temperature at which maximum density is attained is derived from the graph (which is similar to the one shown in Fig. 2 in Section 3.2.1). The piece is then sintered, following the cycle indicated above, at the maximum density temperature. The maximum densification temperatures ranged from 1140 to 1280 $^{\circ}\text{C}$.

Experiments were also performed to examine the influence of peak firing temperature, in which the industrial spray-dried powder was used as a starting composition, and firing temperatures were used both below and above the typical range (1180–1220 $^{\circ}\text{C}$) used for porcelain tiles in industrial practice. The test temperatures were as follows: 1140, 1160, 1180, 1200, 1220, 1240 and 1260 $^{\circ}\text{C}$. In every case, the firing cycle conditions were the same as above.

After firing, the test specimens were polished in a laboratory polishing machine with diamond paste containing particles measuring 1 μm in size, polishing for 30 min, as described elsewhere.⁸

The crystalline phases (quartz and mullite) present were analysed quantitatively by XRD (Philips PW1850), using linear calibration by a procedure described elsewhere.⁷ Specimen microstructure was characterised on polished sections by SEM (Philips XL30). Bulk porosity was determined on polished sections using image analysis software (Olympus MicroImage) linked to an optical microscope. Eighty bright-field images with a magnification of 20 \times were obtained for each sample with enhanced contrast to reveal the pores. The image analysis software then calculated the cross-sectional area occupied by the pores, as well as the pore size distribution.

Gloss was determined on the polished surfaces with a reflectometer (Statistical Novo-gloss, Rhopoint Instruments) with a 60 $^{\circ}$ angle of incidence. Ten gloss measurements were

made on each sample and the arithmetic mean and standard deviation calculated. A roughness meter (Hommelwerke T8000) was also used to make topographic maps of polished surfaces to observe changes in porosity.⁸

The stain resistance of the polished surfaces was determined by staining with an indelible felt pen, followed by cleaning with ethanol at set intervals. This process was repeated until the specimen colour remained constant. The surface colour parameter ΔE^* was determined after surface staining and after each cleaning stage. As reported in the literature,^{3,5} ΔE^* (the difference in colour between the test specimen before staining and during the cleaning process) decreases as cleaning time increases, stabilising after 5 min. The final value, ΔE_F^* , represents the irreversible stain retention (i.e. the stain that cannot be removed by the cleaning process) and is an indirect measure of the product's stain resistance, such that a lower ΔE_F^* value means higher stain resistance.

Fracture strength and Young's modulus were determined by three-point bending tests on the prism-shaped test specimens. Fracture toughness (K_{IC}) was also determined by three-point bending tests on specimens in which a flat notch had been made to a depth of about 40% of the specimen thickness. At least ten specimens were tested for each experimental condition and mechanical property, and the results were averaged.

3. Results and discussion

3.1. Quartz content in fired samples

Fig. 1(a) and (b) show the results of the quantitative measurements of quartz content in the fired bodies by XRD, for the samples fired at their maximum densification temperature. Composition A (see Table 1), to which no quartz was added, contained 14.6 wt% quartz in its starting composition from the other ingredients. As Fig. 1(a) shows, most of the quartz in the starting composition (64–85%) remained undissolved, as a result of the rapid firing cycle (~60 min). As previously reported, a linear relation was obtained between the quartz content in the fired specimens and the level in the starting compositions.⁷ This indicates that for compositions with the same quartz particle size, the quartz dissolution rate at maximum densification temperature does not depend significantly on quartz content. For simplicity, quartz content added to the starting composition (as indicated in Table 1) is used in the following discussion, instead of the actual level in the final sintered material.

In contrast, the rate of dissolution of quartz into the glass phase was somewhat influenced by quartz particle size, despite the fact that the specimens were fired at different temperatures to reach maximum densification. This is because smaller quartz grains dissolve more rapidly than larger grains, owing to their greater surface area. For the range of quartz particle size investigated, the quantity of quartz that remained

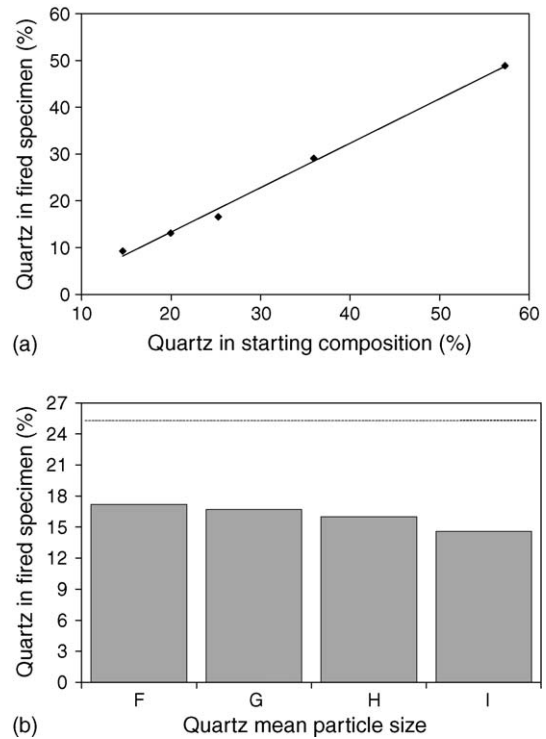


Fig. 1. Relation between quartz content in fired specimens, determined by XRD: (a) quartz content in the starting composition (with constant quartz particle size), compositions A–E; (b) quartz mean particle size, compositions F–I (the broken line indicates the constant quartz content in the starting composition).

undissolved varied between 58% and 68% of the starting amount. For mean quartz particle sizes above about 20 μm (i.e. for compositions F and G) the dissolution rate showed little significant variation.

3.2. Influence of firing temperature

3.2.1. Microstructure and apparent porosity

Fig. 2 shows the influence of firing temperature on the porosity of the samples obtained from the industrial powder, as determined by image analysis. As set out in Section

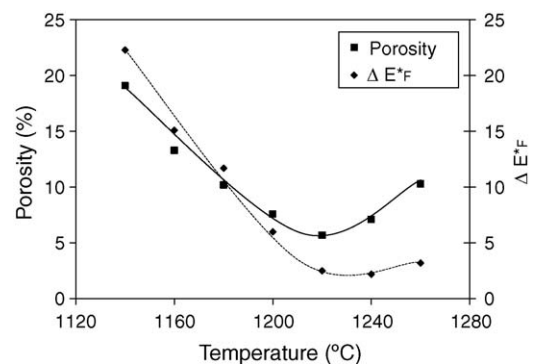


Fig. 2. Influence of firing temperature on porosity and irreversible stain retention (evaluated as ΔE_F^*) for samples obtained from the as-received industrial powder.

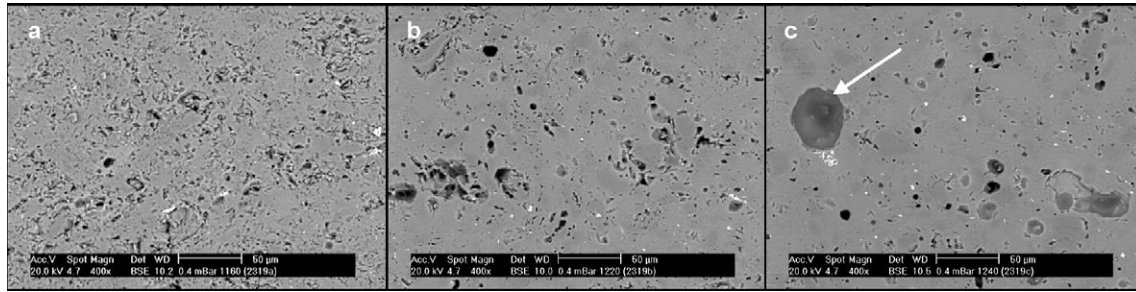


Fig. 3. SEM micrographs of three samples fired at (a) 1160 °C; (b) 1220 °C and (c) 1240 °C obtained from the as-received industrial powder.

2.1, an as-received industrial powder was used in this part of the study on the influence of firing temperature. As expected for liquid-phase sintering, increasing the firing temperature caused a decrease in porosity,^{7,9} Porosity exhibits a minimum value for firing temperatures from around 1210 to 1220 °C (T_{MIN}). Further increase above T_{MIN} leads to an increase in porosity, though now the pores were round and isolated, characteristic of an overfired condition. Fig. 3 shows SEM micrographs of three specimens fired at 1160 °C (below T_{MIN}), 1220 °C (close to T_{MIN}) and 1240 °C (above T_{MIN}). They show that at lower temperature the sample is characterised by an interconnected porous structure, which then evolves at higher temperatures into a more compact matrix containing isolated closed pores. The largest pores are typically 15–20 μm in diameter; however, pores can be even larger in overfiring specimens as marked by the arrow in Fig. 3.

3.2.2. Surface properties

Fig. 2 also shows the variation of ΔE_{F}^* (irreversible stain retention) with firing temperature. ΔE_{F}^* varies in a similar way to porosity, showing a minimum at a temperature slightly above T_{MIN} . The fact that ΔE_{F}^* does not increase above T_{MIN} in the same way as porosity is because, as Fig. 3 shows, the microstructure has changed from a matrix with irregularly shaped interconnected pores to a much more compact matrix with isolated round pores, which are easier to clean. For this reason, in industrial practice it is preferable to fire at a slightly higher temperature than T_{MIN} in order to avoid the

pronounced drop in stain resistance (i.e. rise in ΔE_{F}^*) which results from underfiring.

On the other hand, as is readily observed in Fig. 4, the gloss level of a highly polished sample falls linearly with increase in porosity. The maximum attainable gloss depends on the microstructure of the material, which is defined by its composition and processing conditions. These findings are consistent with the literature on the influence of industrial polishing on porcelain tile gloss.^{8,10} These studies indicate that when the polishing process can completely eliminate surface defects (which is readily achievable in laboratory-scale polishing with micrometre-sized diamond paste), both the tile roughness, and its gloss, will depend solely on the apparent porosity of the piece after polishing.

3.2.3. Mechanical properties

Fig. 5 shows the variation of specimen mechanical properties (fracture strength σ_{R} , modulus of elasticity, E , and toughness, K_{IC}) with firing temperature. All three properties show similar trends with firing temperature, and parallels can be drawn with the trend in sintered density, as easily deduced from porosity variation shown in Fig. 2. For the same starting composition, these mechanical properties all depend on the porosity of the fired piece, and therefore reach their peak values at the firing temperature which gives minimum porosity (1210 °C). Higher temperatures lead to specimen bloating, resulting in reduced strength and other mechanical properties. The fracture toughness values shown in Fig. 5 are consis-

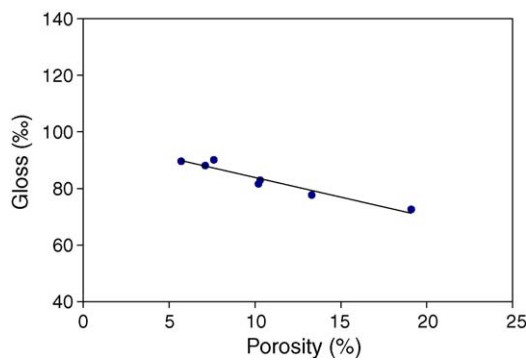


Fig. 4. Relationship between samples porosity and gloss after laboratory polishing, for specimens fired at different peak firing temperatures obtained from the as-received industrial powder.

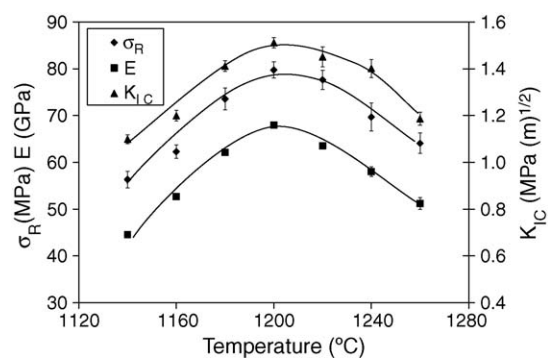


Fig. 5. Relation between mechanical properties (fracture strength σ_{R} , modulus of elasticity E , and toughness K_{IC}) and firing temperature for specimens obtained from the as-received industrial powder.

tent with the fact that most silicate glasses have a fracture toughness of less than $1 \text{ MPa m}^{1/2}$; the crystalline microconstituents of porcelain tiles therefore evidently increase the fracture resistance of the glassy matrix.

Further to be noted is the parallel between toughness and fracture strength, stemming from the significant microstructural heterogeneity of this type of specimen. Indeed, as the micrographs in Fig. 3 show for three specimens fired at different temperatures, even at maximum densification temperature, porosity in the porcelain tiles is significant, with mean pore sizes typically below $15 \mu\text{m}$. Such microstructural heterogeneity affects the mechanical behaviour of the matrix, even though the defects – mainly consisting of pores, but also of cracks related to undissolved quartz grains (as discussed further below) – do not act as critical crack-initiating flaws owing to their small size. Interconnected matrix fracture occurs though, forming the fracture path. In other words, the fracture strength of the porcelain tiles is a consequence of the effect of microstructure on toughness, but not on critical flaw size. This parallelism between K_{IC} and mechanical strength in relation to porosity can only occur in these materials if critical flaw size is much larger than the existing cracks, as reported in.⁷ In that paper the authors reported that the critical flaw size in porcelain tiles was larger than $100 \mu\text{m}$. If we assume that critical flaw size plays a secondary role in fracture, the mechanism that explains fracture in this type of material (and, hence, the parallelism between the mechanical properties in relation to porosity) is that of interconnected matrix fracture, as set out in the literature.^{7,9,11}

3.3. Influence of starting composition

3.3.1. Microstructure and apparent porosity

Fig. 6 shows topographic maps corresponding to the surfaces of some of the compositions with different quartz con-

tents and quartz particle size, together with their porosity values (P). These maps show the major effect of quartz content and particle size on final porous texture. For the sake of simplicity only four specimens corresponding to the extreme compositions are shown in Fig. 6. The other compositions followed the same trend exhibited by these topographic maps. As the quantity of quartz increases in the composition, both pore size and volume grow.⁷ This is because at maximum densification temperature, the quantity of quartz that dissolves in the glassy phase during firing (and hence the quantity of undissolved quartz in the fired tiles) is proportional to the quartz content in the starting composition, as indicated above. The increase in the quantity of undissolved quartz impairs body sinterability. On the other hand, the viscosity of the arising liquid phase influences sinterability much less than the quantity of liquid phase, because when the different specimens are sintered at their maximum densification temperature, liquid-phase viscosity tends to equalise in all the cases, as set out in.⁷

Fig. 6 also shows that raising the quartz particle size increases porosity, as also occurred with the rise in initial quartz content. As discussed in Section 3.1 above, increasing the quartz particle size leads to a higher undissolved quartz content, which lowers the sinterability of the body. However, there is a limit to the effect of quartz particle size on tile final porosity, as shown in Fig. 7. For quartz particles larger than about $30 \mu\text{m}$, the size no longer affects porosity, because quartz dissolution in the glassy phase stabilises when the particles are sufficiently large.

3.3.2. Surface properties

As expected from the relationship between initial quartz particle size and as-fired porosity (Fig. 7), gloss was found to diminish as quartz particle size increased for particle sizes below $30 \mu\text{m}$, and tended to level off for sizes exceeding

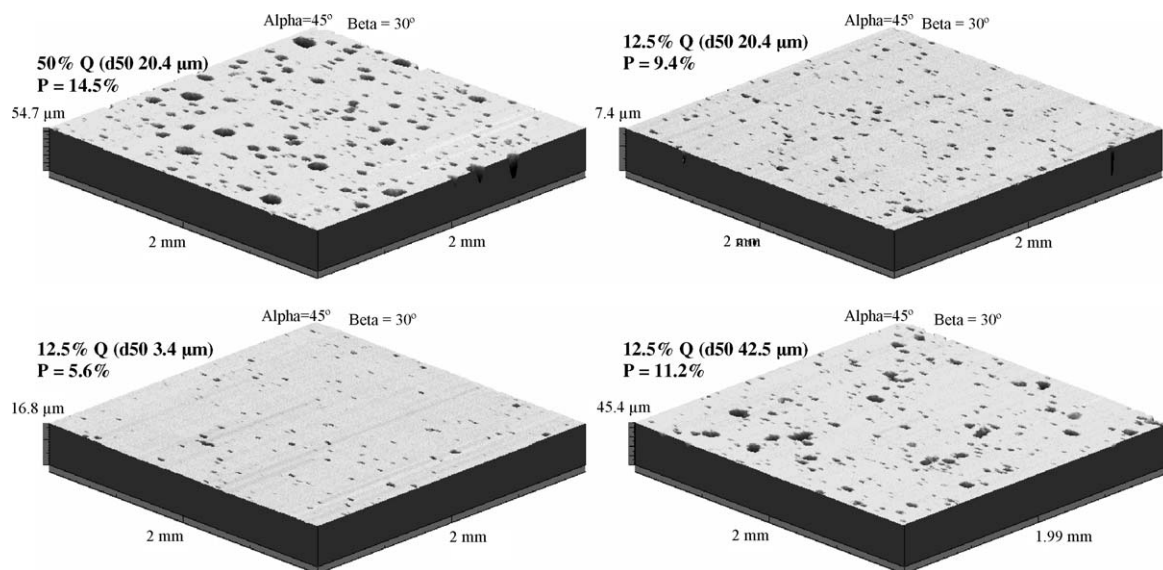


Fig. 6. Topographic maps for samples with different quartz contents and particle sizes as shown. Values of porosity P are also indicated for each sample. Samples are as follows: top left E, top right C, bottom left I and bottom right F.

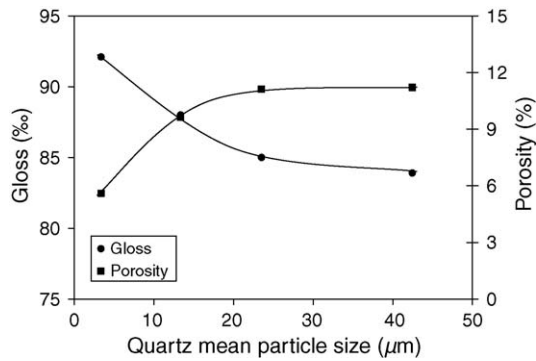


Fig. 7. Variation of gloss and porosity with quartz particle size in the starting composition, for compositions F–I.

this value. These data are also plotted in Fig. 7. Similarly, as the quantity of quartz increases in the composition, both pore size and volume grow (as evidenced by the topographic maps in Fig. 6), significantly reducing gloss. Therefore, when gloss is plotted against porosity for the specimens with different quartz contents and particle size (Fig. 8), all the points lie close to the same curve, despite the simplicity of using porosity as the sole descriptive parameter for such a highly complex property as microstructure. This suggests that for ‘ideal’ polishing (as performed under laboratory conditions), the gloss level is controlled by surface porosity, and is effectively independent of the tile’s composition. Extrapolation of this result to the industrial polishing process must also take into account the surface defects resulting from the polishing operation itself.⁸

Stain resistance (expressed by the parameter, ΔE_F^*) for samples that have been sintered to maximum density also depends exclusively on porosity, independently of how the porosity is produced, as shown in Fig. 8.

However, the dependences of gloss and stain resistance on porosity are not linear, but exhibit a stronger variation for porosity values above about 8–10%. This is probably because, as the topographic maps in Fig. 6 indicate, the surfaces of highly porous specimens (samples E and F) are characterised by larger-sized, irregular pores, which would more

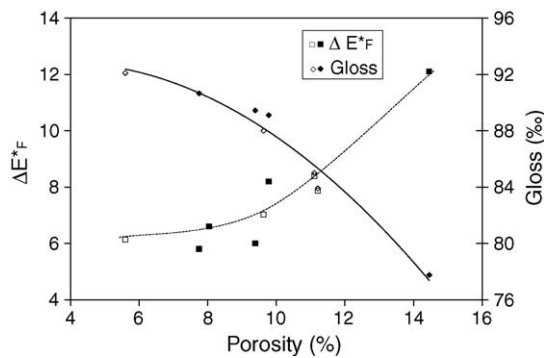


Fig. 8. Relationship between surface properties (gloss and parameter, ΔE_F^*) and porosity for samples with different quartz contents (solid symbols) and quartz mean particle sizes (open symbols). Samples A–I.

significantly degrade both properties. However, this suggested explanation needs to be confirmed by further research.

These results indicate that at standard firing temperatures, the polished surface quality (gloss and stain resistance) depends on tile microstructure, which is in turn related to the starting composition (quartz content) and processing conditions (i.e. quartz particle size reduction by milling). It is therefore not surprising that products with very different qualities can be found in the market-place, associated with highly varied microstructural characteristics.

3.3.3. Mechanical properties

The mechanical properties are plotted against porosity in Fig. 9 for the compositions with different quartz contents and particle sizes. As noted above, mechanical properties are very sensitive to porosity. Both fracture strength and Young’s modulus decrease as porosity increases. Toughness shows a similar trend, but the spread of the data is greater. On the other hand, a clear parallel can again be observed between toughness and fracture strength, which confirms the analysis set out above.

The toughening effect of increased quartz content reported by some researchers for porcelains,^{12,13} or more recently for porcelain tile compositions,⁹ was not observed in this work (Fig. 9(a)). This is because when quartz is added to the starting composition, the resulting microstructural alteration (porosity) predominates over any toughening mechanism ascribable to undissolved quartz particles. The earlier studies did not

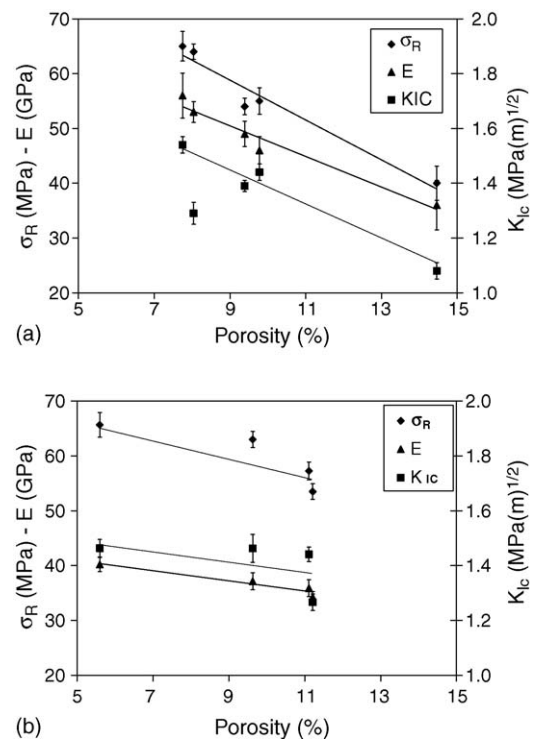


Fig. 9. Relationship between mechanical properties and porosity: (a) compositions with different quartz contents, samples A–E; (b) compositions with different quartz particle sizes, compositions F–I.

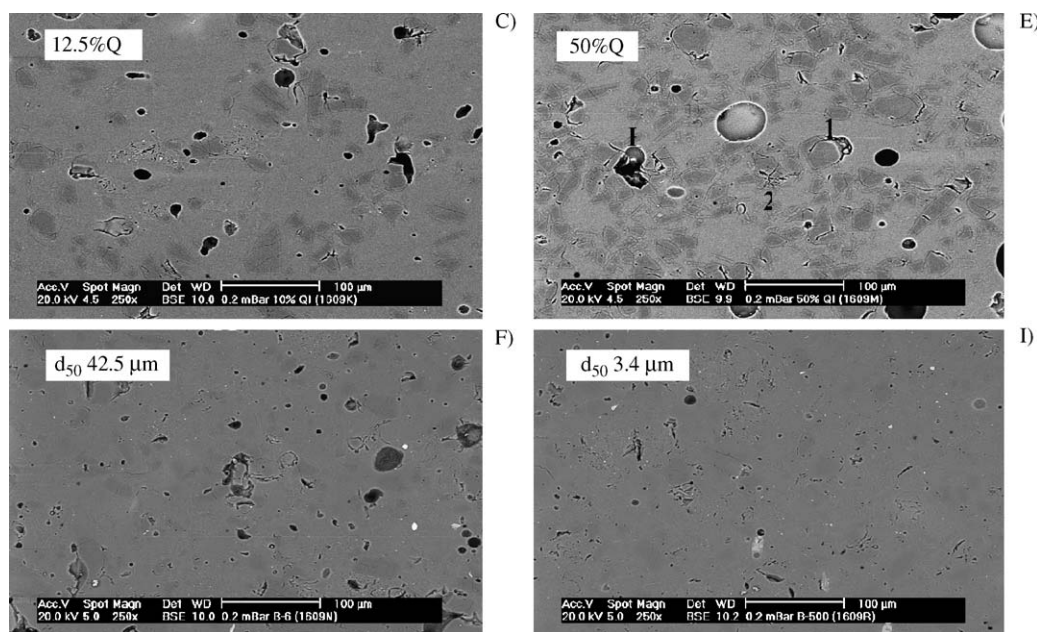


Fig. 10. Microstructures of samples with different quartz contents and particle sizes. The compositions are indicated by the code letters which refer to Tables 1 and 2.

consider the effect of the change in quartz content (or quartz particle size) on final porosity, which the present work shows to be of great importance. Thus, as the micrographs of specimens C (12.5% quartz) and E (50% quartz) in Fig. 10 show, raising the quartz content increases the microstructural heterogeneity, clearly raising porosity and pore size (marked P in Fig. 10(E)), as well as the number of peripheral (1 in Fig. 10(E)) and internal cracks (2 in Fig. 10(E)) caused by undissolved and stressed quartz grains.^{14,15} This microstructural modification decreases toughness, with a quantitatively similar reduction in fracture strength.

The variation of mechanical properties with porosity for the compositions with different quartz particle sizes (Fig. 9(b)) shows a qualitatively analogous tendency to that observed with quartz content, albeit of smaller magnitude (i.e. the slopes of the straight lines are lower). The reason for this difference lies in the smaller microstructural change caused by the rise in quartz particle size compared with quartz content. Thus, increasing the quartz particle size potentially decreases the number of particles in the dispersed phase. This leads to a lower concentration of microstructural defects in the fired body, which tends to constrain interconnected matrix fracture. This can be readily observed in Fig. 10 by comparing the micrographs of specimen F (largest quartz particle size) with I (smallest quartz particle size), and F with E (largest quartz content). Although the micrographs could be clearer, they show that specimen E has a significantly poorer microstructure than specimen F, even though the latter obviously also contains large pores. This suggests that when porosity is the same, quartz content has a greater effect on mechanical properties than quartz particle size, an assumption that needs to be confirmed by further experimentation.

Ekberg et al.¹¹ reached similar conclusions by examining the effects of quartz content and particle size on the mechanical properties of a traditional feldspar porcelain. When the distance between the quartz particles is large, which in practice means lower quartz content, or when porosity and pore diameter decrease, which in practice means smaller quartz particle size, cracks surrounding the quartz particles have less tendency to combine into long continuous cracks, and the result is an increased fracture strength thanks to the decreased actual defect size. Finally, the linear variation observed between fracture strength and porosity in this series of experiments indicates that over the range studied, quartz particle size does not affect the type of fracture that causes failure, in contrast to the effect reported by some researchers for porcelain compositions.¹⁴

4. Conclusions

- Porcelain tile specimens with different microstructures were produced by varying the peak firing temperature for a standard industrial tile composition. Closed porosity was minimised for temperatures around 1210 °C and increased above this temperature in accordance with a typical liquid-phase sintering mechanism. Surface quality, evaluated in terms of gloss and stain resistance, showed an inverse correlation with porosity and hence also depended on firing temperature. The mechanical properties (fracture strength, Young's modulus and toughness) all varied in a similar way with firing temperature, reaching peak values for a temperature close to that for minimum porosity. The correlation between toughness and fracture strength suggests that the critical flaw size for fracture is much

greater than that of the defects observed by microstructural examination.

- Increasing the quartz particle size or content in the starting composition increased the porosity in the fired samples significantly, and gave poorer surface quality. This was consistent with a strong dependence of gloss and stain resistance on polished surface porosity.
- Modifying the quartz content in the starting composition resulted in fired specimens with a wide range of mechanical properties. Mechanical properties (fracture strength, Young's modulus and toughness) decreased when porosity rose, demonstrating the strong dependence of mechanical behaviour on microstructure. Changes in quartz particle size, as in quartz content, affected mechanical properties and porosity in a similar way. However, for the same variation in fired tile porosity, changes in quartz content led to a greater variation in mechanical properties than changes in quartz particle size.
- The results show that the surface and mechanical properties of polished porcelain tile depend predominantly on tile microstructure, which is in turn related to the starting composition and processing conditions.

Acknowledgements

The present study was conducted within the project "Polishcoverings", reference CRAFT-1999-70904 and contract number GIST-CT-2002-50190, funded by the European Commission in the Fifth Framework Programme "Competitive and Sustainable Growth".

References

1. Biffi, G., Il gres porcellanato: manuale di fabbricazione e tecniche di impiego, Faenza editrice, Faenza, 1997.
2. Sánchez, E., Technical considerations on porcelain tile products and their manufacturing process. Part I. *Interceramic*, 2003, **52**(1), 6–15.
3. Beltrán, V., Ferrer, C., Bagán, V., Sánchez, E., García, J. and Mestre, S., Influence of pressing powder characteristics and firing temperature on the porous microstructure and stain resistance of porcelain tile. *Ceram. Acta*, 1996, **8**(4–5), 37–51.
4. Rastelli, E., Tucci, A., Esposito, L. and Selli, S., Stain resistance of porcelain stoneware tile: mechanisms of penetration of staining agents and quantitative evaluation. *Ceram. Acta*, 2002, **14**(1), 30–37.
5. Sánchez, E., Technical considerations on porcelain tile products and their manufacturing process. Part II. *Interceramic*, 2003, **52**(3), 132–139.
6. Hutchings, I. M., Xu, Y., Sánchez, E., Ibáñez, M.J. and Quereda, M.F., Porcelain tile microstructure: implications for polishability. *J. Eur. Ceram. Soc.*, in press.
7. Sánchez, E., Orts, M. J., García-Ten, J. and Cantavella, V., Porcelain tile composition effect on phase formation and end products. *Am. Ceram. Soc. Bull.*, 2001, **80**(6), 43–49.
8. Sánchez, E., García-Ten, J., Ibáñez, M. J., Orts, M. J., Cantavella, V., Sánchez, J. et al., Porcelain tile polishing. I. Wear mechanism. *Am. Ceram. Soc. Bull.*, 2002, **81**(9), 50–54.
9. Leonelli, C., Bondioli, F., Veronesi, P., Romagnoli, M., Manfredini, T., Pellacani, G. C. et al., Enhancing the mechanical properties of porcelain stoneware tiles: a microstructural approach. *J. Eur. Ceram. Soc.*, 2001, **21**, 785–793.
10. Esposito, L. and Tucci, A., Porcelain stoneware tile surfaces. *Am. Ceram. Soc. Bull.*, 2000, **79**(5), 59–63.
11. Ekberg, I. L., Persson, M. and Carlsson, R., Strength improvements of a traditional feldspar porcelain by defect minimization. *Fortschrit-berichte der DKG*, 1992, **7**(1), 247–254.
12. Bradt, R. C., The toughness of porcelain: a high-tech approach to a traditional ceramic. In *Proceedings of the Arita fine ceramics symposium*, 1986, pp. 15–22.
13. Carty, W. M. and Senapati, U., Porcelain: raw materials, processing, phase evolution and mechanical behavior. *J. Am. Ceram. Soc.*, 1998, **81**(1), 3–20.
14. Warsaw, S. I. and Seider, R., Comparison of strength of triaxial porcelains containing alumina and silica. *J. Am. Ceram. Soc.*, 1967, **50**(7), 337–343.
15. Carty, W. M. and Pinto, B. M., Effect of filler size on the strength of porcelain bodies. *Ceram. Eng. Sci. Proc.*, 2002, **23**(2), 95–105.